Revised version, 10 August 2006

Arsenic incorporation into FeS_2 pyrite and its influence on dissolution: a DFT study

Marc Blanchard[a], Kate Wright[b], C. Richard A. Catlow[a]

[a] Royal Institution of Great Britain, 21 Albemarle Street, London W1S 4BS, UK

[b] Nanochemistry Research Institute, Department of Applied Chemistry, Curtin University of Technology, P.O. Box U1987, Perth 6845, Western Australia

Communicating Author: Marc Blanchard

e-mail: marc@ri.ac.uk

Tel.: +44-20-74092992

Fax: +44-20-76702920

Abstract

FeS_2 pyrite can incorporate large amounts of arsenic (up to ca. 10 wt %) and hence has a strong impact on the mobility of this toxic metalloid. Focussing on the lowest arsenic concentrations for which the incorporation occurs in solid solution, the substitution mechanisms involved have been investigated by assuming simple incorporation reactions in both oxidising and reducing conditions. The solution energies were calculated by Density Functional Theory (DFT) calculations and we predict that the formation of AsS dianion groups is the most energetically favourable mechanism. The results also suggest that the presence of arsenic will accelerate the dissolution and thus the generation of acid drainage, when the crystal dissolves in oxidising conditions.

Keywords: arsenic, pyrite, DFT

1. Introduction

Iron-bearing sulphide minerals are largely responsible for the generation of acid mine drainage and hence the release of toxic metals such as arsenic into the environment. FeS_2 pyrite, the most common iron sulphide mineral, can incorporate large amounts of arsenic (up to ca. 10.0 wt.%, Abraitis et al., 2004) within its structure. In addition, these arsenian pyrites often contain minor and trace elements including valuable metals such as gold (e.g. Abraitis et al., 2004). It is therefore important to understand the crystal setting and speciation of arsenic in the pyrite bulk structure. Despite extensive study of this system, the arsenic incorporation mechanism in arsenian pyrite remains a matter of debate.

FeS_2 pyrite crystallizes in the cubic symmetry (space group Pa3) with four formula units per unit cell. Each iron atom is coordinated by six sulphurs in a slightly distorted octahedron and each sulphur atom is bonded to three Fe atoms and its S_2 dianion group (Fig. 1). All iron and all sulphur sites are equivalent. The structure is fully defined by two parameters: the unit cell length, a_0 = 5.416 Å and the sulphur fractional coordinate, u = 0.385 (Brostigen and Kjekshus, 1969; Finklea et al., 1976). As a result of the structural differences between pyrite and arsenopyrite (FeAsS, orthorhombic) or löllingite ($FeAs_2$, orthorhombic) there is no extensive solid solution between the phases. The highest arsenic concentrations in pyrite may represent metastable solid solutions, but in other cases, arsenic is incorporated within the pyrite lattice by atomic substitution. It has generally been proposed that arsenic substitutes for sulphur, forming either AsS or AsAs dianion groups. The X-ray absorption spectroscopic studies (X-ray Absorption Near Edge Structure and Extended X-ray Absorption Fine Structure) favour the former possibility with arsenic in the same local configuration as in arsenopyrite (Foster et al., 1998; Simon et al., 1999; Savage et al., 2000). As for the oxidation state, these techniques indicate the presence of arsenic as As^0 (Foster et al., 1998) or As^{-I}

(Simon et al., 1999; Savage et al., 2000). Tossel et al. (1981) used molecular orbital theory to calculate the electronic structure of arsenopyrite. They proposed that the best description of the dianion is AsS (-II), with an oxidation number of both sulphur and arsenic of -I, in agreement with EXAFS data. However a nominal charge of -3 for the AsS dianion group has also been advanced to explain the fact that arsenian pyrite is a p-type semiconductor in contrast with the n-type semiconducting properties of other pyrite crystals. Alternatively, Chouinard et al. (2005) have recently suggested that arsenic can also be incorporated as a cation, substituting for Fe^{2+}. Their chemical study of auriferous pyrite from a high-sulfidation deposit has shown a concentric and sectoral zonation of arsenic and silver, which would suggest a coupled substitution for iron, i.e. one As^{3+} and one Ag^{+} substituting for two Fe^{2+}. From a computational point of view, Reich and Becker (2006) have investigated the thermodynamic mixing properties of arsenic into pyrite and marcasite using first-principles and Monte Carlo calculations. Assuming that arsenic substitutes for sulphur to form AsS dianion groups, they determined that 6 wt. % is the maximum solubility of arsenic in iron disulfides.

In this paper, we investigate the incorporation of arsenic in FeS_2 pyrite using electronic structure calculations. The different structural configurations of arsenic are discussed by comparing the calculated solution energies of incorporation reactions in two different redox conditions. The structural and electronic properties of the most energetically favourable configuration are then described and the implications for dissolution of pyrite discussed.

2. Methodology

Our calculations were performed using the density functional theory code CASTEP (Segall et al., 2002), within which the wavefunctions are expanded in plane waves. Only the valence

electrons were considered explicitly through the use of ultrasoft pseudopotentials (Vanderbilt, 1990). Von Oertzen et al. (2005) have shown that the gradient corrected exchange-correlation functionals give the best results for the unit cell as well as the electronic structure of FeS_2 pyrite. We adopted this approximation and more specifically, we used the revised Perdew-Burke-Ernzerhof functional (Hammer et al., 1999).

Boundary conditions in CASTEP are periodic in all three dimensions and we are interested here in pyrite crystals displaying low arsenic concentrations (below 5 wt. % As). Therefore the calculations were performed on 2x2x2 pyrite supercells (i.e. 96 atoms) containing up to two arsenic atoms. Considering the size of the system, only calculations at the Γ-point of the Brillouin zone with an energy cut-off of 400 eV were affordable. However, these parameters lead to a satisfactory convergence of the total energy of less than 9 meV per atom compared to the use of a higher energy cut-off (600 eV) and a denser k-point grid (2 × 2 × 2 Monkhorst-Pack k-point grid). The incorporation of arsenic atoms into the diamagnetic FeS_2 pyrite involves the presence of unpaired electrons and possibly electron transfer. In order to find the ground state, the calculations were set up with a high initial value of the total spin (i.e. number of unpaired electrons in the system assuming several high-spin iron ions around the arsenic for instance), which was optimised during the geometry relaxation.

The comparison of the different geometric configurations of arsenic requires specification of the incorporation reactions for which the solution energies have been determined. Thus the total energies of all the relevant compounds were needed and were calculated following geometry optimisation, with the same level of accuracy as described above and with approximately the same number of atoms as for the periodic systems (i.e. between 80 and 100 atoms). For molecules or single atoms, a box of 20x20x20 $Å^3$ was built and was checked to be sufficient for the convergence of the total energy, which ensured that the energy differences are meaningful and not distorted by different levels of accuracy.

3. Results

3.1. Energetic Study

Arsenic has been successively substituted in iron and sulphur sites in 2x2x2 pyrite supercells. Because of the presence of S_2 dianion groups, we have investigated the following three species for the substitution of sulphur: formation of AsS groups, formation of As_2 groups and substitution of one As atom for one S_2 group.

Relatively simple reactions are used to model two redox conditions. Starting with oxidizing conditions, arsenic is incorporated by reaction of pyrite with arsenolite (As_2O_3). Each of the four following reactions corresponds to a different substitution type:

One As substituting for one Fe:

$$Fe_{32}S_{64} + 1/2\ As_2O_3 \rightarrow Fe_{31}AsS_{64} + 1/2\ Fe_2O_3, \quad (1)$$

One AsS unit substituting for one S_2 unit:

$$Fe_{32}S_{64} + 1/2\ As_2O_3 + 1/4\ O_2 \rightarrow Fe_{32}S_{63}As + SO_2, \quad (2)$$

One As substituting for one S_2 unit:

$$Fe_{32}S_{64} + 1/2\ As_2O_3 + 5/4\ O_2 \rightarrow Fe_{32}S_{62}As + 2\ SO_2, \quad (3)$$

One As_2 unit substituting for one S_2 unit:

$$Fe_{32}S_{64} + As_2O_3 + 1/2\ O_2 \rightarrow Fe_{32}S_{62}As_2 + 2\ SO_2. \quad (4)$$

The calculated total energies of each component are listed in Table 1. As expected, the most stable form of the dioxygen molecule (O_2) was found to be the triplet electronic state and calculated bond lengths for O_2 and SO_2 are within 2.5 % of those measured for the gas phase (CRC Handbook 2002-2003). Several magnetic structures have been probed for hematite (Fe_2O_3). The lowest energy corresponds to the antiferromagnetic structure, as is known from

experimental observations. The relaxed lattice parameters are in satisfactory agreement with the experimental values (Blake et al, 1966) with discrepancies of 0.2 and 1.8 % for the a and c parameters respectively. Arsenolite (As_2O_3) is a molecular crystal, which can be described by As_4O_6 cages held together by van der Waals forces. Its modelling by DFT-methods is therefore problematic. We chose to fix the unit cell to its experimental value, i.e. 11.0734 Å (Ballirano and Maras, 2002) and to relax only the internal coordinates. For substitution reaction 3, two different configurations of $Fe_{32}S_{62}As$, were considered. In the first, the sulphur vacancy is located in the same dianion unit as the substituting arsenic atom, while in the second, the vacancy is present in a dianion unit adjacent to the arsenic (Table 1). The first configuration, with the arsenic replacing one S_2 unit has, as expected, the lower energy and was then used in reaction 3. The solution energies for reactions 1-4 are given in Table 2.

Our results show that arsenic incorporation is energetically more favourable on the sulphur rather than the iron site. Moreover, it seems slightly more favourable to substitute arsenic for a whole S_2 group than for only a sulphur atom although the energy of reactions (2) and (3) are sufficiently close for both processes to be feasible. However the As_2 configuration is clearly less favourable. We checked that use of the fixed unit cell of arsenolite introduces only a small uncertainty into the results of the calculations (i.e. a positive shift smaller than 0.35eV for all reactions) and does not change these conclusions.

To gain further insight into the lowest solution energy that corresponds to the replacement of two sulphur atoms by one arsenic atom, we investigate the formation of a sulphur vacancy in both pure and arsenian pyrite. Keeping the redox conditions identical as in reactions 1 to 4, the creation of a sulphur vacancy can be written as follows:

$$Fe_{32}S_{63}As + O_2 \rightarrow Fe_{32}S_{62}As + SO_2, \quad (5)$$

$$Fe_{32}S_{64} + O_2 \rightarrow Fe_{32}S_{63} + SO_2. \quad (6)$$

The energy cost to remove the sulphur atom from the AsS group is -0.328 eV (reaction 5), while the energy needed to create a sulphur vacancy at an infinite distance from the arsenic atom is the same as in pure pyrite (reaction 6), i.e. -0.204 eV. These energies suggest that in arsenian pyrite, the formation of a sulphur vacancy will preferentially occur next to the arsenic atom rather than far away from it; they also show that the creation of sulphur vacancies is an exothermic process, suggesting that it is thermodynamically favoured for pyrite to dissolve in these oxidizing conditions, in good agreement with what is observed in nature (e.g. Smedley and Kinniburgh, 2002) thereby supporting our model; although we should note that we are not necessarily implying that the dissolution mechanism involves formation of sulphur vacancies. In addition, it is interesting to note that the presence of arsenic will favour the formation of sulphur vacancies, and hence dissolution. This important result has implications for environmental studies of acid rock drainage generation.

It is worth considering in more detail, why there is an energetic preference for one arsenic atom substituting for an S_2 group compared to one arsenic atom substituting for one sulphur atom, which could be explained to a first approximation by the larger radius (by ~ 15 %) of arsenic compared to sulphur; or it could be due to the dissolution of pyrite in these conditions. We have already shown that it is energetically favourable to create sulphur vacancies in this material under oxidising conditions, so the formation of a single As substituting for one S_2 group can be seen as reflecting our prediction that pyrite dissolves under these conditions.

We now turn to arsenic incorporation under reducing and anoxic conditions that is modelled by reaction of pyrite with realgar (AsS). Reactions 7 to 10 correspond to the four substitution types and are analogous to reactions 1 – 4.

One As substituting for one Fe:

$$Fe_{32}S_{64} + AsS \rightarrow Fe_{31}AsS_{64} + FeS, \quad (7)$$

One AsS unit substituting for one S_2 unit:

$Fe_{32}S_{64} + AsS \rightarrow Fe_{32}S_{63}As + 1/4\ S_8$, (8)

One As substituting for one S_2 unit:

$Fe_{32}S_{64} + AsS \rightarrow Fe_{32}S_{62}As + 3/8\ S_8$, (9)

One As_2 unit substituting for one S_2 unit:

$Fe_{32}S_{64} + 2\ AsS \rightarrow Fe_{32}S_{62}As_2 + 1/2\ S_8$. (10)

The crystal structure of realgar (AsS), mackinawite (FeS) and sulphur (S_8) all include a contribution of van der Waals forces, and as for arsenolite (As_2O_3), the cells were fixed to the experimental values during the energy calculation (Mullen and Nowacki, 1972 for realgar; Lennie et al., 1995 for mackinawite; Rettig and Trotter, 1987 for sulphur). The solution energies are given in Table 2 and show that substitution will occur at sulphur rather than iron sites, as for the oxidising case. The substitution of one arsenic atom for one S_2 group is not energetically favoured, which is explained by the fact that under reducing conditions pyrite precipitates rather than dissolves and no sulphur can be removed. In reactions 7 - 10 above, sulphur is oxidized from -II to 0 in S_8, expressing slightly reducing conditions. An alternative set of reactions has also been considered where the arsenic source corresponds to the arsenic hydride AsH_3. In these purely reducing conditions, the results are qualitatively the same with the same relative order of the solution energies, as the formation of AsS units favoured.

Thus according to the results as a whole, arsenic will be located preferentially in sulphur sites where it is more energetically favourable to form AsS groups than As_2 groups in pure FeS_2 pyrite under conditions in which the mineral is stable. We will now focus on this most stable configuration. Up to two arsenic atoms have been incorporated in the 2x2x2 pyrite supercell, which allows us to assess approximately the concentration effect on the substitution energy. For this purpose the substitution reaction of the first arsenic atom for one sulphur atom can be written as follows:

$Fe_{32}S_{64} + As_{(g)} \rightarrow Fe_{32}S_{63}As + S_{(g)}$ (11)

The energies of $As_{(g)}$ and $S_{(g)}$ have been approximated by the total energies of the neutral atoms in large empty boxes (Table 1). The substitution costs 1.103 eV.

The incorporation of the second arsenic atom into this supercell corresponds to the following reaction:

$$Fe_{32}S_{63}As + As_{(g)} \rightarrow Fe_{32}S_{62}As_2 + S_{(g)} \quad (12)$$

The substitution energy is now 1.052 eV when the two arsenic atoms are as distant as possible within the supercell (i.e. ~ 9 Å) and 1.067 eV when the arsenic atoms belong to two neighbouring dianions. Even if the energy of arsenic incorporation seems to decrease slightly when the arsenic concentration increases, the energy difference is too small to draw any firm conclusion concerning a possible clustering of arsenic. Such a clustering is suggested by Savage et al. (2002) from EXAFS spectra performed on pyrite with comparable arsenic concentrations (below 5 wt. %).

3.2. Structural and Electronic Properties of the most energetically favourable arsenic configuration

The relaxed geometry of the arsenian pyrite with AsS groups is shown in Figure 2. Unit cell parameters and interatomic distances are given in Table 3 and are compared with the calculated and experimental values of pure pyrite. The model used here describes the structure of FeS_2 pyrite very well, with a calculated unit cell only 0.2 % smaller than the experimental one and bond distances also in good agreement. For the arsenian pyrite, the substitution induces an expansion of the unit cell proportional to the arsenic concentration. The supercells $Fe_{32}S_{63}As$ and $Fe_{32}S_{62}As_2$ correspond to arsenic concentrations of 1.9 and 3.8 wt % respectively and display expansions of 0.45 % and 0.83 % in volume relative to the calculated values for pure pyrite. This unit cell expansion is actually a consequence of the greater length

of the bonds involving arsenic: the As-S bonds are about 4.6 % longer than S-S bonds while As-Fe bonds are about 2.8 % longer than Fe-S bonds. The As-S and As-Fe interatomic distances are in good agreement with those determined by Savage et al. (2000) from their EXAFS spectra: As-S and Fe-S bonds were reported to be 2.25 and 2.32 Å respectively, for pyrites containing between <0.01 and 1.63 wt % of arsenic. For comparison, the measurements in arsenopyrite give 2.34 and 2.36 Å respectively for the same interatomic bonds (X-ray Diffraction: Fuess et al., 1987; EXAFS: Foster et al., 1998).

Regarding the electronic properties, all calculations were started with a relatively high value of the total spin and in all cases the relaxed structure presents the lowest possible spin state, i.e. one spin up for the substitution of one sulphur by one arsenic atom. However, this spin is delocalized and although this situation is physically unlikely, it will not affect the results deduced from the energies. Our results also indicate that the AsS groups are more negatively charged than S_2 groups and within the AsS unit, sulphur is always more negatively charged than arsenic.

The electronic structure of the pure pyrite, which was studied in more details in Blanchard et al. (2005), is in good agreement with experimental data. Here with the use of a GGA functional associated with ultrasoft pseudopotentials, we also obtain a better description of the band gap, supporting the observations of von Oertzen et al. (2005). The calculated value of 1.0 eV compares well with the experimental value of 0.9 eV (see, e.g. Cervantes et al., 2002). The supercell with one AsS group also shows semiconducting properties (Fig. 3a) with a band gap of about the same size as in pure pyrite. In figure 3a, the partial densities of states (PDOS) lines slightly cross the Fermi level only because of the smearing width used for the integration. This semiconducting characteristic and the fact that the AsS group acts as a defect, which traps electrons agree well with experimental observations that describe arsenian pyrites as a p-type semiconductor (Abraitis et al., 2004). The partial densities of states also

highlight the presence of a strong As-Fe hybridization, which corresponds to the highest valence band. This strong As-Fe interaction is clearly visible on total electron density maps (Fig. 4) where a covalent bond is made between the two atoms. On the other hand, when the arsenic concentration increases, our calculations suggest that the electronic structure changes and becomes metallic with the As-Fe band now located above the Fermi level (Fig 3b).

4. Discussion

In natural environments, processes involving pyrite (precipitation, dissolution) are complex and various. Water is always present and reactions are often bacterially assisted. It is therefore difficult to model accurately, at this level, all components of the system. The reactions considered here have been kept as simple as possible while still incorporating the essential features of the chemistry. By doing so, all energy components can be calculated and no additional experimental data are needed that can introduce extra uncertainties to the calculated solution energies and indeed in many cases such data are not available and therefore must be calculated. Our results provide general insights into arsenic dissolution in pyrite. In conditions where pyrite is stable, arsenic will substitute for sulphur forming AsS dianion groups.

Regarding the oxidation state of arsenic, our population analysis would suggest the presence of As^{I-} rather than As^{0} where the AsS group seems to have a charge more negative than II-. This local configuration is the one put forward by X-ray absorption spectroscopic studies for pyrites extracted from gold mineralizations (Foster et al., 1998; Simon et al., 1999; Savage et al., 2000). However, it has also been shown that pyrite from high-sulfidation deposits, implying highly acidic and oxidizing conditions, incorporates arsenic as cation, i.e. in iron site (Chouinard et al., 2005). Our results rule out this substitution mechanism for the arsenic incorporation in pure FeS_2 pyrite but we do not exclude the possibility that this

substitution could happen in very specific conditions. In the same study, Chouinard et al. (2005) proposed a coupled substitution of arsenic and silver for iron (one As^{3+} and one Ag^{+} substituting for two Fe^{2+}). These pyrite crystals also contain other trace elements like Au, Cu, Se, Te. Thus complex defect reactions involving couples substitutions or other defects, not considered here, could significantly change the behaviour of arsenic.

Finally the conclusions drawn from this work complement and validate the theoretical work made by Reich and Becker (2006). Based on the assumption that arsenic substitutes for sulphur they studied by first-principles and Monte Carlo methods the solubility of arsenic in pyrite and marcasite. They found that up to 6 wt % of arsenic can be incorporated in solid solution in pyrite while beyond this concentration, arsenic segregates into arsenopyrite domains.

The magnitude of the solution energies obtained in oxidising conditions suggest appreciable solubility of arsenic in pyrite; while the higher values calculated for reducing conditions indicate lower solubility in the bulk. Calculations of adsorption energies on the surface of the material would clearly be of interest.

5. Conclusion

Arsenic incorporation as a solid solution into pyrite has been investigated in oxidising and reducing conditions. In both redox conditions, it is more energetically favourable to substitute arsenic for sulphur rather than for iron. Moreover the formation of AsS groups is favoured compared to As_2 group. The very local configuration is then very close to the one in arsenopyrite. During the dissolution of pyrite, the formation of sulphur vacancies will preferentially occur in the neighbouring of arsenic. The presence of this metalloid could hence have an accelerating effect on pyrite dissolution with the environmental consequences that

implies. Further work would be required in order to determine the actual oxidation state of arsenic.

Acknowledgements. This work was funded by NERC via the grant NER/T/S/2001/00855 and NE/C515704/1. We thank M. Alfredsson and J. Brodholt for their helpful discussions.

References

Abraitis P. K., Pattrick R. A. D. and Vaughan D. J. (2004) Variations in the compositional, textural and electrical properties of natural pyrite: a review. *Int. J. Miner. Process.* **74**, 41-59.

Ballirano P. and Maras A. (2002) Refinement of the crystal structure of arsenolite, As_2O_3. *Z. Kristallogr. NCS* **217**, 177-178.

Blanchard M., Alfredsson M., Brodholt J., Price G. D. , Wright K. and Catlow C. R. A. (2005) Electronic structure study of the high-pressure vibrational spectrum of FeS_2 pyrite. *J. Phys. Chem. B* **109**, 22067-22073.

Blake R. L., Hessevick R. E., Zoltai T. and Finger L. W. (1966) Refinement of the hematite structure. *Am. Miner.* **51**, 123-129.

Brostigen G. and Kjekshus A. (1969) Redetermined crystal structure of FeS2 (pyrite). *Acta Chem. Scand.* **23**, 2186-2188.

Cervantes P., Slanic Z., Bridges F., Knittle E. and Williams Q. (2002) The band gap and electrical resistivity of FeS_2-pyrite at high pressures. *J. Phys. Chem. Solids* **63**, 1927-1933.

Chouinard A., Paquette J. and Williams-Jones A. E. (2005) Crystallographic controls on trace-element incorporation in auriferous pyrite from the Pascua epithermal high-sulfidation deposit, Chile-Argentina. *The Can. Miner.* **43**, 951-963.

C. R. C. Handbook of Chemistry and Physics (2002-2003) ed. D. R. Lide, 83rd edn. CRC Press.

Finklea S. L., Cathey L. and Amma E. L. (1976) Investigation of the bonding mechanism in pyrite using the Mößbauer effect and X-ray crystallography. *Acta Crystallogr*. **32A**, 529-537.

Foster A. L., Brown Jr G. E., Tingle T. N. and Parks G. A. (1998) Quantitative arsenic speciation in mine tailings using X-ray absorption spectroscopy. *Am. Miner*. **83**, 553-568.

Fuess H., Kratz T., Töpel-Schadt J. and Miehe G. (1987) Crystal structure refinement and electron microscopy of arsenopyrite. *Z. Kristallogr*. **179**, 335-346.

Hammer B., Hansen L. B. and Norskov J. K. (1999) Improved adsorption energetics within density-functional theory using revised Perdew-Burke-Ernzerhof functionals. *Phys. Rev. B* **59**, 7413-7421.

Lennie A. R., Redfern S. A. T., Schofield P. F. and Vaughan D. J. (1995) Synthesis and Rietveld crystal structure refinement of mackinawite, tetragonal FeS. *Mineral. Mag*. **59**, 677-683.

Mullen D. J. E. and Nowacki W. (1972) Refinement of the crystal structures of realgar AsS and orpiment, As2S3. *Z. Kristallogr., Kristallgeometrie, Krystallphysik, Krystallchemie* **136**, 48-65.

Reich M. and Becker U. (2006) First-principles calculations of the thermodynamic mixing properties of arsenic incorporation into pyrite and marcasite. *Chem. Geol*. **225**, 278-290.

Rettig S. J. and Trotter J. (1987) Refinement of the structure of orthorhombic sulphur, alpha - S8. *Acta Crystallogr. C* **43**, 2260-2262.

Savage K. S., Tingle T. N., O'Day P. A., Waychunas G. A. and Bird D. K. (2000) Arsenic speciation in pyrite and secondary weathering phases, Mother Lode Gold District, Tuolumne County, California. *Appl. Geochem*. **15**, 1219-1244.

Segall M. D., Lindan P. J. D., Probert M. J., Pickard C. J., Hasnip P. J., Clark S. J. and Payne M. C. (2002) First-principles simulation: ideas, illustrations and the CASTEP code. *J. Phys.: Cond. Matt*. **14**, 2717-2743.

Simon G., Huang H., Penner-Hahn J. E., Kesler S. E. and Kao L.-S. (1999) Oxidation state of gold and arsenic in gold-bearing arsenian pyrite. *Am. Miner*. **84**, 1071-1079.

Smedley P. L. and Kinniburgh D. G. (2002) A review of the source, behaviour and distribution of arsenic in natural waters. *Appl. Geochem*. **17**, 517-568.

Tossel J. A., Vaughan D. J. and Burdett J. K. (1981) Pyrite, Marcasite, and Arsenopyrite type minerals: Crystal chemical and structural principles. *Phys. Chem. Minerals* **7**, 177-184.

Vanderbilt D. (1990) Soft self-consistent pseudopotentials in a generalized eigenvalue formalism. *Phys. Rev. B* **41**, 7892-7895.

Von Oertzen G. U., Jones R. T. and Gerson A. R. (2005) Electronic and optical properties of Fe, Zn and Pb sulfides. *Phys. Chem. Minerals* **32**, 255-268.

Tables

Table 1

Calculated total energies of all components involved in reactions 1-12

Formula	Description	Total energy (eV)
$Fe_{32}S_{64}$	Pyrite supercell	-45570.1940
$Fe_{32}S_{63}$	Sulphur vacancy	-45289.0758
	Pyrite supercell with:	
$Fe_{31}AsS_{64}$	• 1 As substituting for 1 Fe	-44873.4064
$Fe_{32}S_{63}As$	• 1 AsS unit substituting for 1 S_2 unit	-45463.4710
$Fe_{32}S_{62}As$	• 1 As substituting for 1S_2 unit	-45182.4767
$Fe_{32}S_{62}As$	• 1 AsS unit substituting for 1 S_2 unit + 1 S vacancy	-45182.3574
$Fe_{32}S_{62}As_2$	• 2 AsS units substituting for 2 S_2 units	-45356.7948
$Fe_{32}S_{62}As_2$	• 1 As_2 unit substituting for 1 S_2 unit	-45356.2408
$As_{32}O_{48}$	Arsenolite unit cell	-26498.6810
$Fe_{40}O_{60}$	Hematite supercell	-60871.5020
$As_{48}S_{48}$	Realgar supercell	-21642.0688
$Fe_{48}S_{48}$	Mackinawite supercell	-54982.6650
S_{96}	Sulphur supercell	-26711.2056
O_2	Oxygen molecule	-870.3752
SO_2	Sulphur dioxide molecule	-1151.6978
S	Sulphur atom	-275.4882
As	Arsenic atom	-169.8644

Table 2

Calculated solution energies for reactions under oxidising (1-4) and reducing (7-10) conditions

Reactions (see text)	Solution energies (eV)
1	3.084
2	0.703
3	0.374
4	1.913
7	2.192
8	1.116
9	3.869
10	2.739

Table 3

Calculated unit cell paramater (a_0) and interatomic distances for pure FeS_2 pyrite and the arsenian pyrite containing AsS groups

	Obs.	$Fe_{32}S_{64}$	$Fe_{32}S_{63}As$ with 1AsS group	$Fe_{32}S_{62}As_2$ with 2 AsS groups
a_0	5.416	5.406	5.414	5.421
S-S	2.158	2.188	2.186 - 2.210	2.187 - 2.216
As-S	/	/	2.288	2.287
Fe-S	2.264	2.256	2.220 - 2.270	2.225 - 2.274
Fe-As	/	/	2.320	2.324

Observed data are from Brostigen and Kjekshus (1969).

Figure captions

Fig. 1 Unit cell of FeS_2 pyrite. Iron and sulphur atoms are in black and white respectively.

Fig. 2 Relaxed structure of the $Fe_{32}S_{63}As$ supercell containing the AsS group. The Fe-S bonds have been omitted for clarity sake. Arsenic atom (medium grey) is labelled.

Fig. 3 Partial densities of state of the arsenian pyrite supercells containing one and two AsS groups (a and b respectively). Iron DOS have been normalised to one atom.

Fig. 4 Total electron density map of the $Fe_{32}S_{63}As$ supercell containing the AsS group. The (110) plane passing through Fe-(S,As) and S-(S,As) bonds is represented here. The scale is given in electrons/$Å^3$.

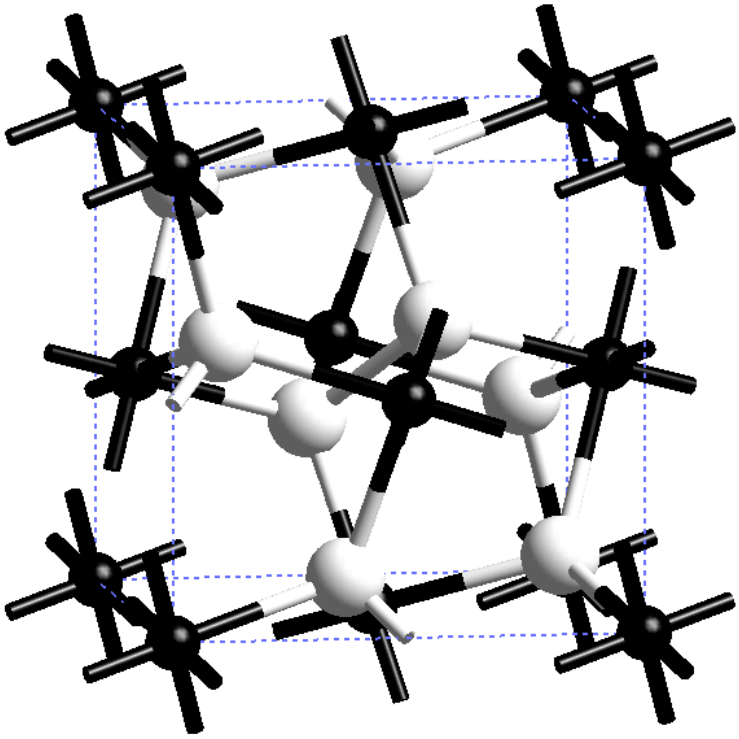

Fig. 1 Unit cell of FeS_2 pyrite. Iron and sulphur atoms are in black and white respectively.

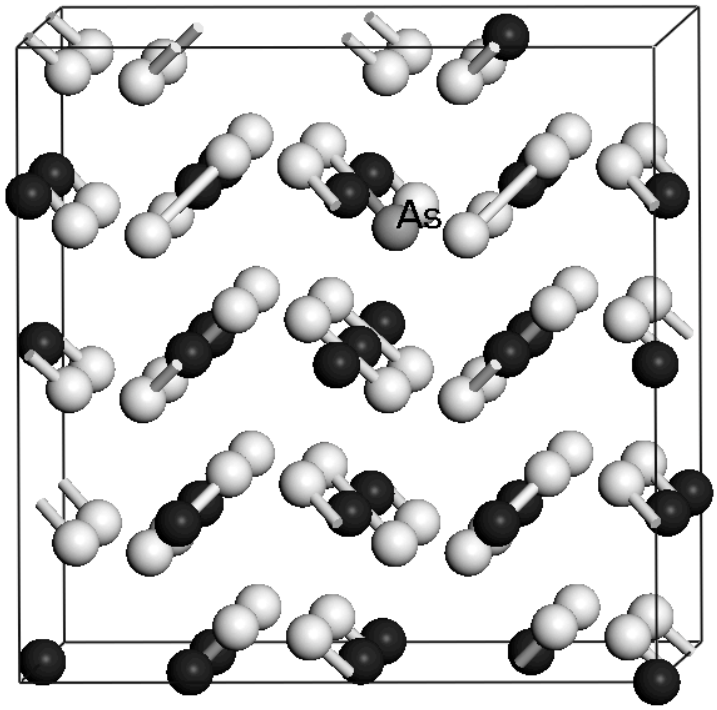

Fig. 2 Relaxed structure of the $Fe_{32}S_{63}As$ supercell containing the AsS group. The Fe-S bonds have been omitted for clarity sake. Arsenic atom (medium grey) is labelled.

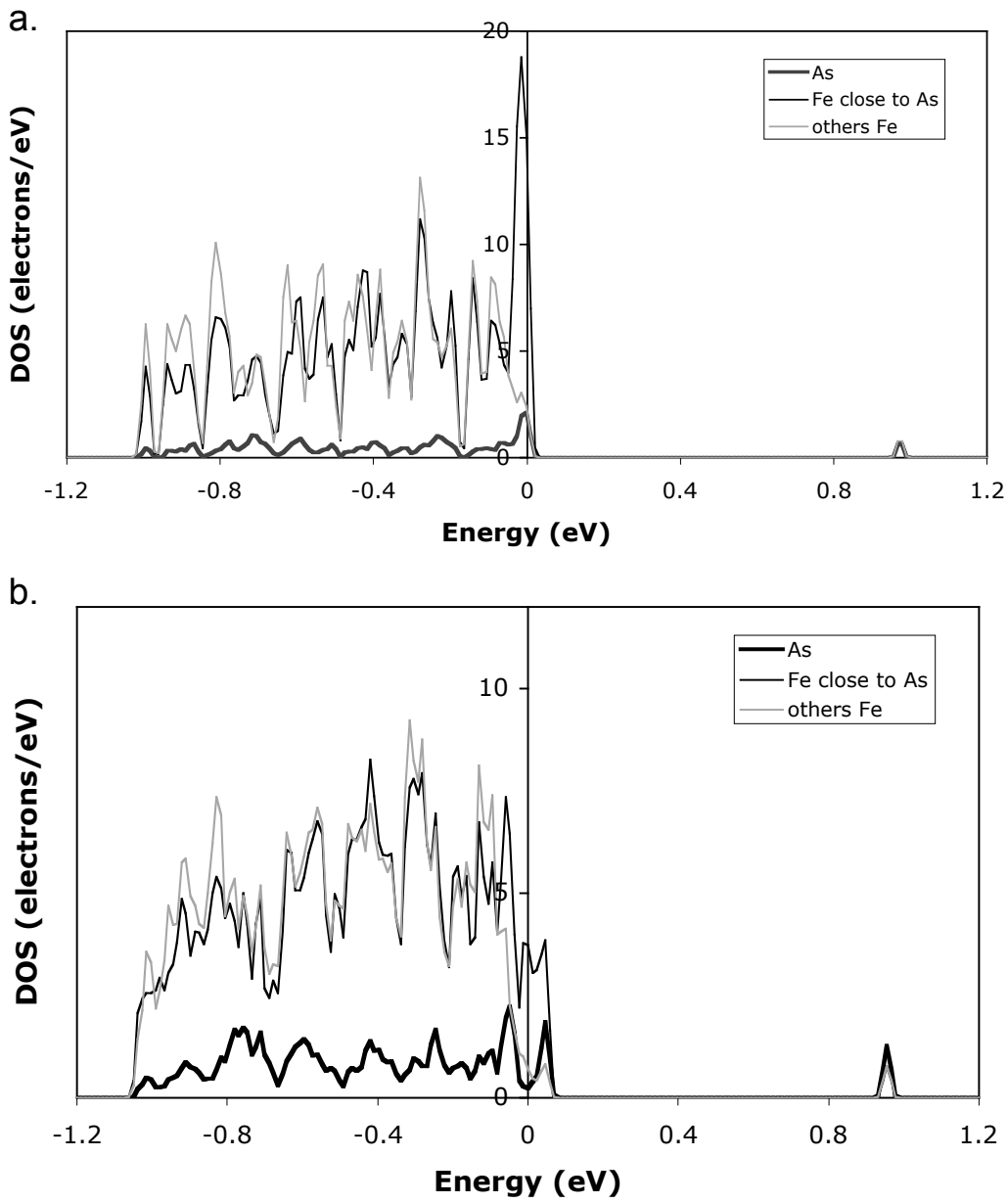

Fig. 3 Partial densities of state of the arsenian pyrite supercells containing one and two AsS groups (a and b respectively). Iron DOS have been normalised to one atom.

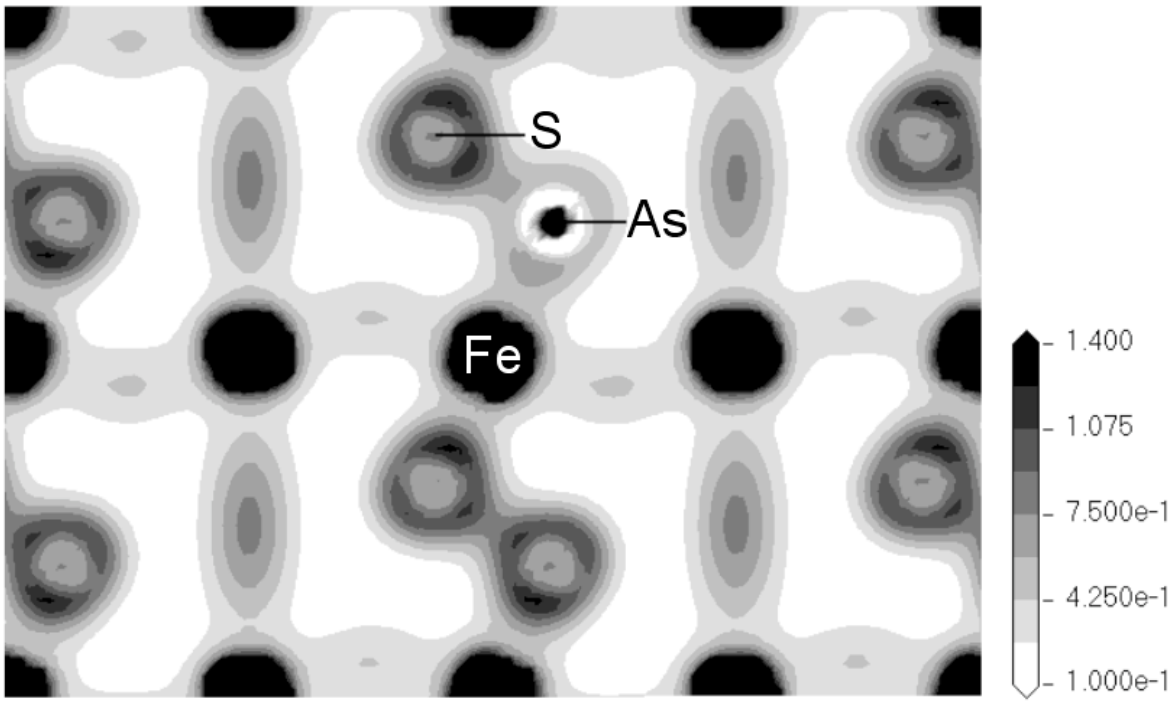

Fig. 4 Total electron density map of the $Fe_{32}S_{63}As$ supercell containing the AsS group. The (110) plane passing through Fe-(S,As) and S-(S,As) bonds is represented here. The scale is given in electrons/$Å^3$.